Glycobiology, vol. 20 no. 4 pp. 473–484, 2010
doi:10.1093/glycob/cwp199
Advance Access publication on December 15, 2009

A polysaccharide, MDG-1, induces $S1P_1$ and bFGF expression and augments survival and angiogenesis in the ischemic heart

Shuo Wang[2,3], Zhang Zhang[3], Xiao Lin[2], De-Sheng Xu[4], Yi Feng[1,2], and Kan Ding[1,3]

[2]Engineering Research Center of Modern Preparation Technology of TCM, Shanghai University of Traditional Chinese Medicine, Pudong, Shanghai, 201203, People's Republic of China; [3]Glycochemistry & Glycobiology Lab, Shanghai Institute of Materia Medica, Chinese Academy of Sciences, Pudong, Shanghai, 201203, People's Republic of China; and [4]Shuguang Hospital, Shanghai University of Traditional Chinese Medicine, Shanghai 201203, People's Republic of China

Received on June 6, 2009; revised on November 10, 2009; accepted on December 10, 2009

Ophiopogon japonicus **is a traditional Chinese medicine used to treat cardiovascular disease. Recent studies have confirmed its beneficial properties, but not the mechanism of action. Herein, we investigate the anti-ischemic properties of a water-soluble β-D-fructan (MDG-1) from *Ophiopogon japonicus*, and assess the cytoprotective and proangiogenic effects of MDG-1. MDG-1 protects cardiomyocyte and microvascular endothelial cells (HMEC-1) against oxygen glucose deprivation (OGD)-induced cell death, as well as protect myocardial cells from ischemia-induced death occurring after coronary artery ligation in rats. Meanwhile, MDG-1 stimulates the differentiation of HMEC-1 cells into capillary-like structures in vitro and functions as a chemoattractant in migration assays, and promotes neovascularization in ischemic myocardium. In addition, MDG-1 upregulates sphingosine kinase 1 and sphingosine-1-phosphate (S1P) receptor 1 expression. Both MDG-1 and S1P induce basic fibroblast growth factor (bFGF) expression in HMEC-1 cells. Further study revealed that both MDG-1 and S1P induce Akt and ERK phosphorylation in a dose- and time-dependent manner, an effect that is attenuated by pre-treatment with either the Akt inhibitor wortmannin or the ERK inhibitor PD98059, and MDG-1 can also induce eNOS phosphorylation and increases in production of NO. These data indicate that MDG-1 presented remarkable anti-ischemic activity and protects cardiomyocyte and HMEC-1 cells from ischemia-induced cell damage by inducing S1P1 and bFGF cytoprotective and proangiogenic effects via the S1P/bFGF/Akt/ERK/eNOS signaling pathway.**

Keywords: angiogenesis/myocardial ischemia/*Ophiopogon japonicus*/polysaccharide/Sphingosine 1-phosphate

Introduction

Ophiopogon japonicus, widely distributed in Southeast Asia, is a traditional Chinese medicine used to treat cardiovascular diseases for thousands of years. With the exception of clinical evidence of its efficacy, this medicine has been confirmed in various experiments as having anti-ischemia and anti-arrhythmia properties, as well as inhibiting platelet aggregation, protecting the endothelium from apoptosis, and microcirculation improvement (Zhou et al. 2003; Huang et al. 2003). In patients with acute myocardial ischemia, the main therapeutic goals are to minimize myocardial damage, by protecting the cells, and improve tissue repair. Angiogenesis within the myocardial infarct scar will improve cardiac repair (Ware and Simons 1997; Carmeliet 2003). Recent evidence demonstrated that certain compounds can be used therapeutically to stimulate vessel growth in ischemic tissues, a process termed 'therapeutic vasculogenesis' (Luttun et al. 2002). In previous work, data suggested that a water-soluble polysaccharide, MDG-1 (MDG-1 is the same as FOJ-5 which was a compound name in the reference paper (Zheng et al. 2009), while MDG-1 is a drug name in this paper) extracted from *Ophiopogon japonicus* might have an interesting role in anti-myocardial ischemia (Zheng et al. 2009). MDG-1, a β-D-fructan with an average molecular weight of 3400 Da, constitutes approximately 4% of the total plant. MDG-1 contains a backbone composed of Fruf (2→1), and a branch of Fruf (2→6) Fruf (2→per average 2.8 of main chain residues and contains trace of α-D-Glc, which maybe connect to its reducing terminal (Xu et al. 2005) (Figure 1). MDG-1 could protect cardiomyocyte from the damage induced by hypoxia/reoxygenation and restore heart contraction, resume coronary blood flux, and restrain the increasing of heart rate caused by ischemia–reperfusion of isolated rat myocardium (Zheng et al. 2009).

Sphingosine 1-phosphate (S1P), part of an intracellular signaling pathway involved in cell survival and angiogenesis, is critical to the development and therapy of ischemic disease (Maceyka et al. 2002). S1P binds to members of the endothelial differentiation gene (EDG) receptor family, which leads to phosphorylation of both Akt and extracellular signal-regulated kinase (ERK) (Waeber et al. 2004). Phosphorylation, and therefore activation, of these two kinases is implicated in diverse signaling events in cells, including mitosis, apoptosis, cytoskeletal rearrangement, survival, growth, migration, and differentiation (Kennedy et al. 1997; Bullard et al. 2003). The Akt survival pathway is implicated specifically in the anti-apoptotic effect of a variety of treatments in endothelial cells. Recent studies demonstrated that S1P protects hearts against ischemia/reperfusion injury when administered prior to the index ischemia (preconditioning) and mediates myocardial ischemic preconditioning in isolated mouse hearts (Jin et al. 2002, 2004; Vessey et al. 2006). This protection required sphingosine kinase-1 (SPHK1), the key enzyme catalyzing the formation of S1P, and likely depends on exported S1P to initiate a cell survival signaling cascade (Jin et al. 2008). Activation of SPHK1 and S1P receptor 1 ($S1P_1$) is important to prevent apoptosis and promote

[1]To whom correspondence should be addressed: Tel: +86-021-5080-6928; fax: +86-021-5080-6928; e-mail: kding@mail.shcnc.ac.cn and Tel: +86-021-5132-2493; fax: +86-021-5132-2491; e-mail: fyi@vip.sina.com

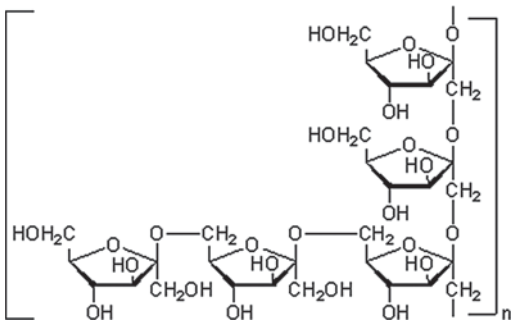

Fig. 1. The repeating unit structure of the MDG-1 from *Ophiopogon japonicus*, and MDG-1 is β-D-fructosan with an average molecular weight of 3400 Da, containing a backbone composed of Fruf (2→1), and a branch of Fruf (2→6) Fruf (2→ per average 2.8 of main chain residues and trace of α-D-Glc, which may be connected to its reducing terminal.

angiogenesis (Lee et al. 1999; Spiegel and Milstien 2003; Miura et al. 2003).

Most studies of polysaccharides are concerned with antitumor activity, immunostimulation, hypoglycemic activity, and other properties of these chemicals. To date, very few polysaccharides from plants display any potential anti-ischemic properties, except MDG-1. In the present study we focused on one possible mechanism for the cytoprotective effect of MDG-1 on human microvascular endothelial cells (HMEC-1), as microvascular endothelium is associated directly in angiogenesis and is distributed widely throughout cardiac tissue, and cardiomyocyte. Our evidence demonstrates that the anti-ischemic effect of MDG-1 might result from its cytoprotective and proangiogenic effects, as the result of activation of the S1P/bFGF/Akt/ERK/eNOS signaling pathway.

Results

MDG-1 protects cardiomyocyte and HMEC-1 cells against OGD-induced cell death

To test whether MDG-1 may cause cytotoxicity in vitro, the effect of MDG-1 on HMEC-1 cell viability was determined using the MTT assay. HMEC-1 cells were treated with or without increasing concentrations of MDG-1 for 24 h. MDG-1 has no significant effect on HMEC-1 cell viability at lower concentrations less than 10 mM (Figure 2A). Only treatment with high concentrations of MDG-1 (20 and 40 mM) reduced cell viability (84.9 ± 3.5% and 77.5 ± 4.6% viability, respectively). Therefore, MDG-1 was only used at concentrations lower than or equal to 10 mM in all subsequent experiments.

We used the LDH assay to assess the effect of MDG-1 on OGD-induced cardiomyocyte and HMEC-1 cell death. For cardiomyocyte cells, without MDG-1 treatment, under OGD conditions, LDH release was 68 ± 2% of the total cellular content. The basal LDH release in normoxic cells was 8 ± 1%. MDG-1 reduced OGD-induced cell death significantly in a dose-dependent manner (Figure 2B). For HMEC-1 cells, without MDG-1 treatment, under OGD conditions, LDH release was 48 ± 1% of the total cellular content. The basal LDH release in normoxic cells was 26 ± 1%. MDG-1 reduced OGD-induced cell death significantly in a dose-dependent manner (Figure 2C). To test whether either Akt or ERK signaling pathway have the role in MDG-1-induced cytoprotection, the cells were pretreated with the Akt inhibitor wortmannin (1 μM) or the ERK inhibitor PD98059 (50 μM) for 1 h and then incubated with MDG-1 under OGD for 8 h. We found that both wortmannin and PD98059 reduce MDG-1-induced cytoprotection, and this cytoprotection effect was abolished by the treatment of wortmannin and PD98059 together (Figure 2D), suggesting that both Akt and ERK signaling pathway involved in the effect of MDG-1 cytoprotection.

MDG-1 promotes HMEC-1 cell migration and tube formation

To examine the effect of MDG-1 on HMEC-1 cell migration, the scratch wound healing assay was employed. As shown in Figure 2E, MDG-1 accelerated the migration of HMEC-1 cells compared to vehicle-treated cells. When cells were pretreated with wortmannin or PD98059 for 1 h, MDG-1-induced migration was reduced significantly suggesting that both Akt and ERK signaling pathway implicated in the effect of MDG-1 on cell migration (Figure 2F).

The initial phase of angiogenesis involves organization of individual endothelial cells into a three-dimensional tube-like structure. Tube-like structures appeared on matrigel after cell culture for 16 h. In addition to increasing microvessel tube length compared to the control (Figure 3A and B), MDG-1 also increased tube branching points (Figure 3A and C). A similar effect on tube length and branching points was observed in cells treated with bFGF (10 ng/ml) and S1P (10 μM; Figure 3A, B and C). However, the ability of MDG-1 to increase tube length and branching points was prevented by wortmannin, PD98059, and Su5402 (Figure 3D and E), suggesting that Akt, ERK, and bFGF signaling pathways are crucial to tube formation induced by MDG-1.

MDG-1 significantly alters the expression of angiogenic cytokines

To test whether MDG-1 exerts its pro-angiogenic effect by altering the expression of angiogenic growth factors, antibody arrays recognizing several cytokines associated with angiogenesis were employed. Expression patterns differed between treatment groups, but revealed modest changes in the expression of the acidic fibroblast growth factor (aFGF) (Figure 4A). However, bFGF levels in HMEC-1 cells were consistently upregulated 5- to 10-fold compared to the controls. Combined with the results of the tube formation assay, these data suggest that bFGF might have an important role in the promotion of tube formation by MDG-1.

MDG-1 increases SPHK1 and $S1P_1$ levels

To test whether MDG-1 activity requires the involvement of SPHK1 and $S1P_1$ in HMEC-1 cells, their protein expressions were determined. HMEC-1 cells were treated with increasing concentrations of MDG-1 for 18 h. SPHK1 protein expression was increased significantly from 229.5 ± 16.2% (0.4 mM) to 289.2 ± 28.7% (10 mM) (Figure 4B). MDG-1 also significantly upregulated $S1P_1$ protein expression from 138.0 ± 18.5% (0.4 mM) to 268.5 ± 20.2% (10 mM) (Figure 4C).

Since MDG-1 upregulated bFGF and activated the S1P signaling pathway, which are both involved in angiogenesis, we examined whether the S1P signaling pathway was required for bFGF expression. HMEC-1 cells were treated with S1P and MDG-1, respectively, for 18 h. Results showed that both S1P

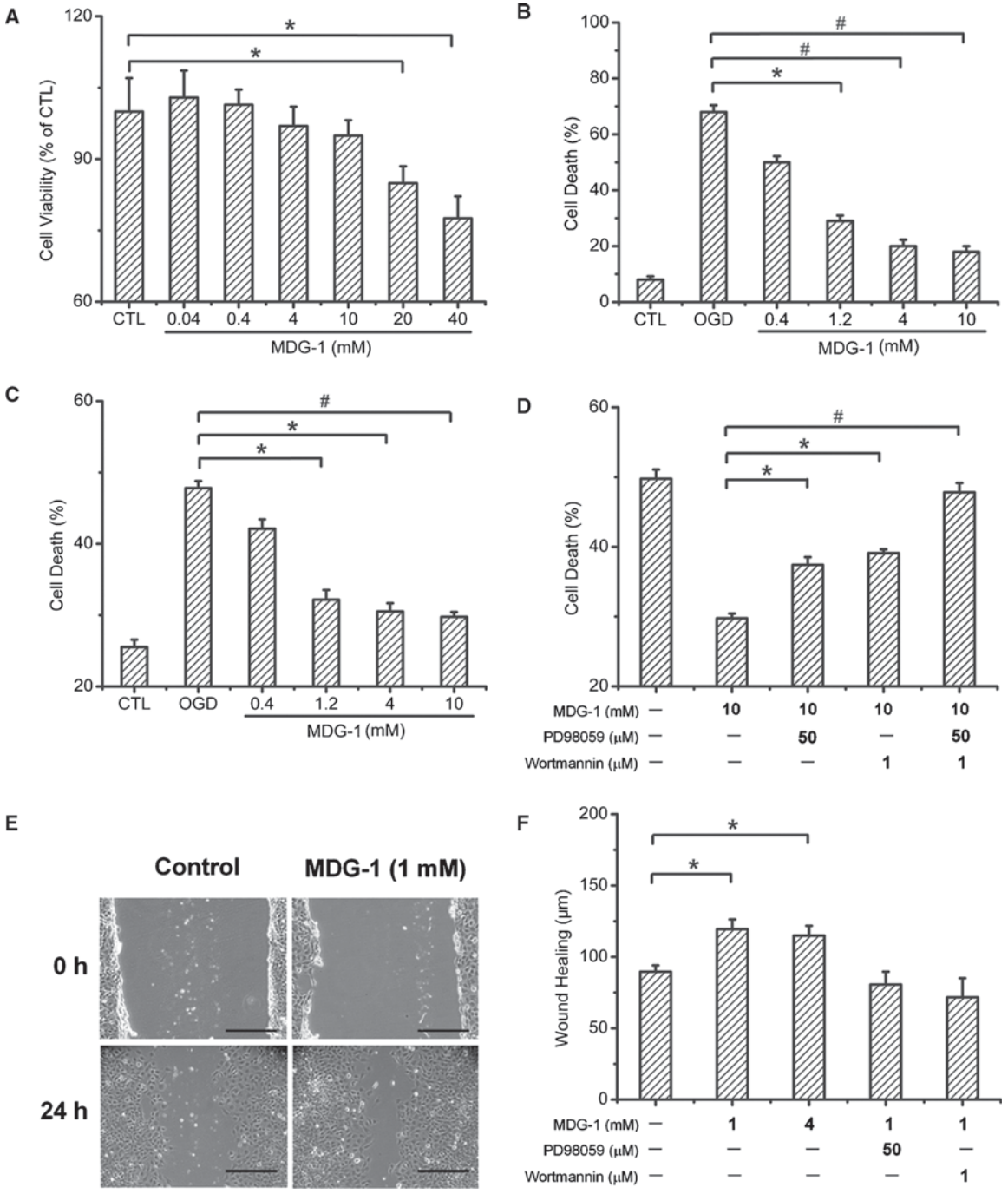

Fig. 2. MDG-1 is not toxic to HMEC-1 cells, protects cells from OGD-induced injury, and promotes endothelial cell migration. (**A**) HMEC-1 cells were treated with increasing concentrations of MDG-1 (0.04, 0.4, 4, 10, 20, and 40 mM) for 24 h, and then assessed for viability using the MTT method as described in *Material and methods*. Cardiomyocyte cells (**B**) or HMEC-1 cells (**C**) were treated with MDG-1 (0.4, 1.2, 4, and 10 mM) under OGD or without MDG-1 in a 5% CO_2 incubator as a control (CTL) for 8 h. LDH released into the medium was detected spectrophotometrically. (**D**) The HMEC-1 cells were pretreated with PD98059 (50 μM) and wortmannin (1 μM), alone or in combination, for 1 h. Then, the cells were maintained in the same medium with or without 10 mM of MDG-1 under ODG for 8 h followed by the LDH assay. (**E**) The scratch wound healing assay of HMEC-1 cells was performed with or without MDG-1 [1 mM or 4 mM (data not shown)] treatment for 0 and 24 h. (**F**) After the scratch, the HMEC-1 cells were treated with MDG-1 (1 mM or 4 mM) in the presence of PD98059 (50 μM) or wortmannin (1 μM) for 24 h. The wound healing distance was measured as described in *Materials and methods*. Data are means ± SD for triplicate experiments ($^{*}P < 0.05$; $^{\#}P < 0.01$).

(1 μM) and MDG-1 (4 mM) upregulated bFGF expression in HMEC-1 cells (Figure 4D). On the other hand, we found that bFGF (10 ng^{-1} mL^{-1}) had no effect on either SPHK1 or $S1P_1$ expression in HMEC-1 cells (data not shown).

MDG-1 increases Akt and ERK phosphorylation

We next investigated whether phosphorylation of Akt and ERK is required for the cytoprotective and pro-angiogenic effect of MDG-1 on HMEC-1 cells. HMEC-1 cells were treated with

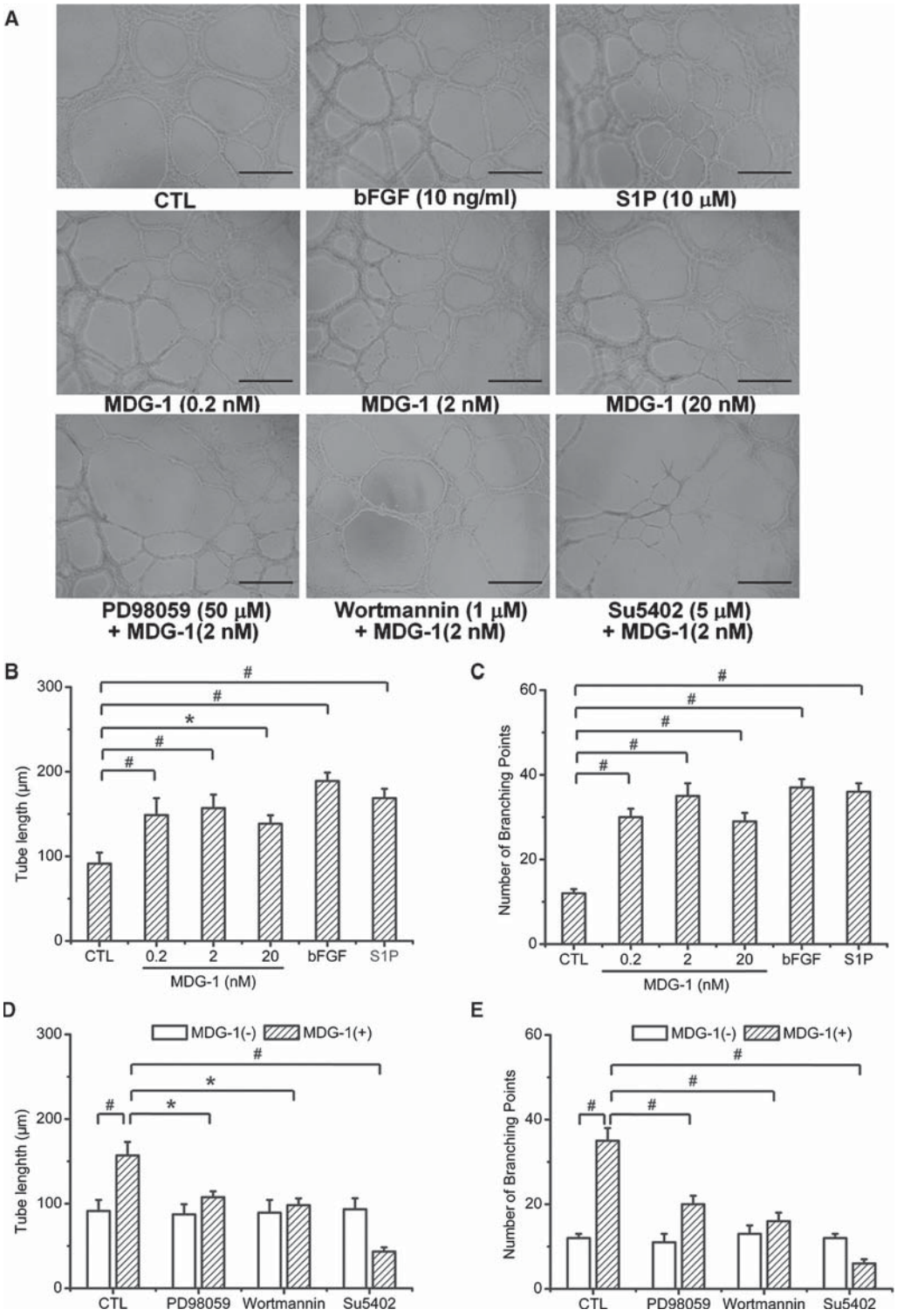

Fig. 3. MDG-1 promotes microvessel tube formation in three-dimensional cell culture. Tube formation was determined 16 h after plating as described in *Materials and methods*. (**A**) Representative micrographs of tube formation of HMEC-1 cells treated with bFGF (10 ng/mL), S1P (10 μM), and MDG-1 (0.2, 2 and 20 nM) in the presence or absence of PD98059 (50 μM), wortmannin (1 μM) or Su5402 (5 μM). (**B**) and (**C**) Statistical analysis of tube length (**B**) and branching points (**C**) of the HMEC-1 cells treated with MDG-1, bFGF, and S1P. (**D**) and (**E**) MDG-1-induced increase in tube length (**D**) and branching points (**E**) was attenuated by PD98059, wortmannin, or Su5402. Data are means ± SD for triplicate experiments ($^{*}P < 0.05$; $^{\#}P < 0.01$).

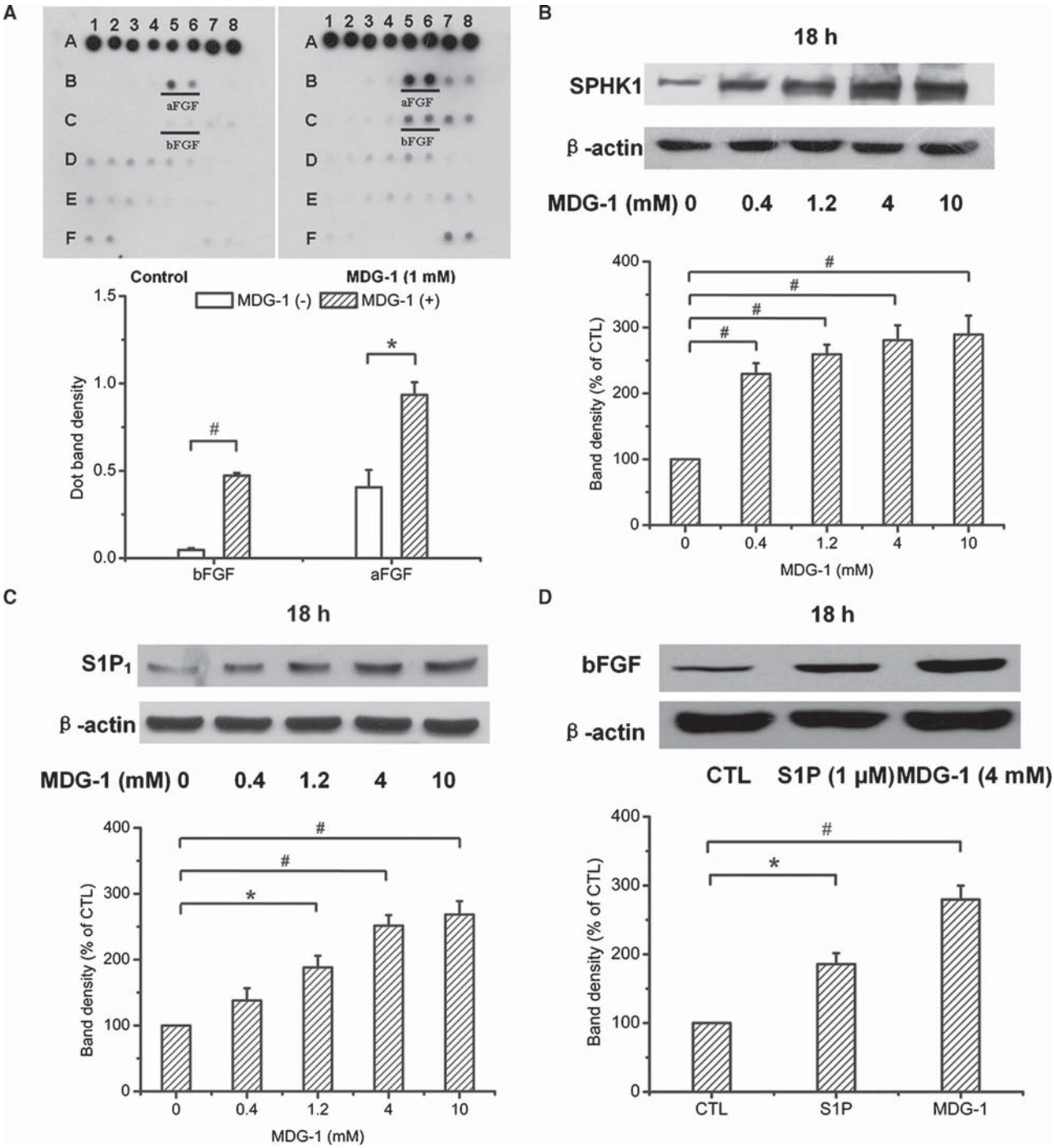

Fig. 4. MDG-1 alters the expression of aFGF and bFGF, increases SPHK1 and $S1P_1$ expression levels, while both S1P and MDG-1 upregulates bFGF expression in HMEC-1 cells. (**A**) HMEC-1 cells maintained in the presence of MDG-1 (1 mM) for 18 h were assessed for angiogenesis using the angiogenesis antibody array according to the manufacturer's instructions. The antibodies were visualized by chemoluminescence and band densities for each blot were shown below the figures. HMEC-1 cells incubated with MDG-1 (0, 0.4, 1.2, 4, and 10 mM) for 18 h were lysed and subjected to Western blotting for the SPHK1 (**B**) and $S1P_1$ (**C**) antibody. HMEC-1 cells incubated with S1P (1 μM) or MDG-1 (4 mM) for 18 h. The cells lysates were detected by Western blotting using the bFGF (**D**) antibody. Band densities are shown below the figures. Data are means ± SD for triplicate experiments ($^{*}P < 0.05$; $^{\#}P < 0.01$).

increasing concentrations of MDG-1 for 1 h. Immunoblotting for Akt revealed that Akt^{Ser473} but not Akt^{Thr308} phosphorylation was increased significantly from 159.7 ± 18.5% (0.4 mM) to 430.4 ± 20.2% (10 mM; Figure 5A). A single dose of MDG-1 (4 mM) induced a time-dependent increase in Akt phosphorylation (Figure 5C). Meanwhile, the results show that MDG-1 induced ERK phosphorylation significantly (Figure 5B). A single dose of MDG-1 (4 mM) induced ERK phosphorylation which peaked at 15 min and lasted until 2 h (Figure 5D). A similar effect on Akt and ERK phosphorylation was observed in cells treated

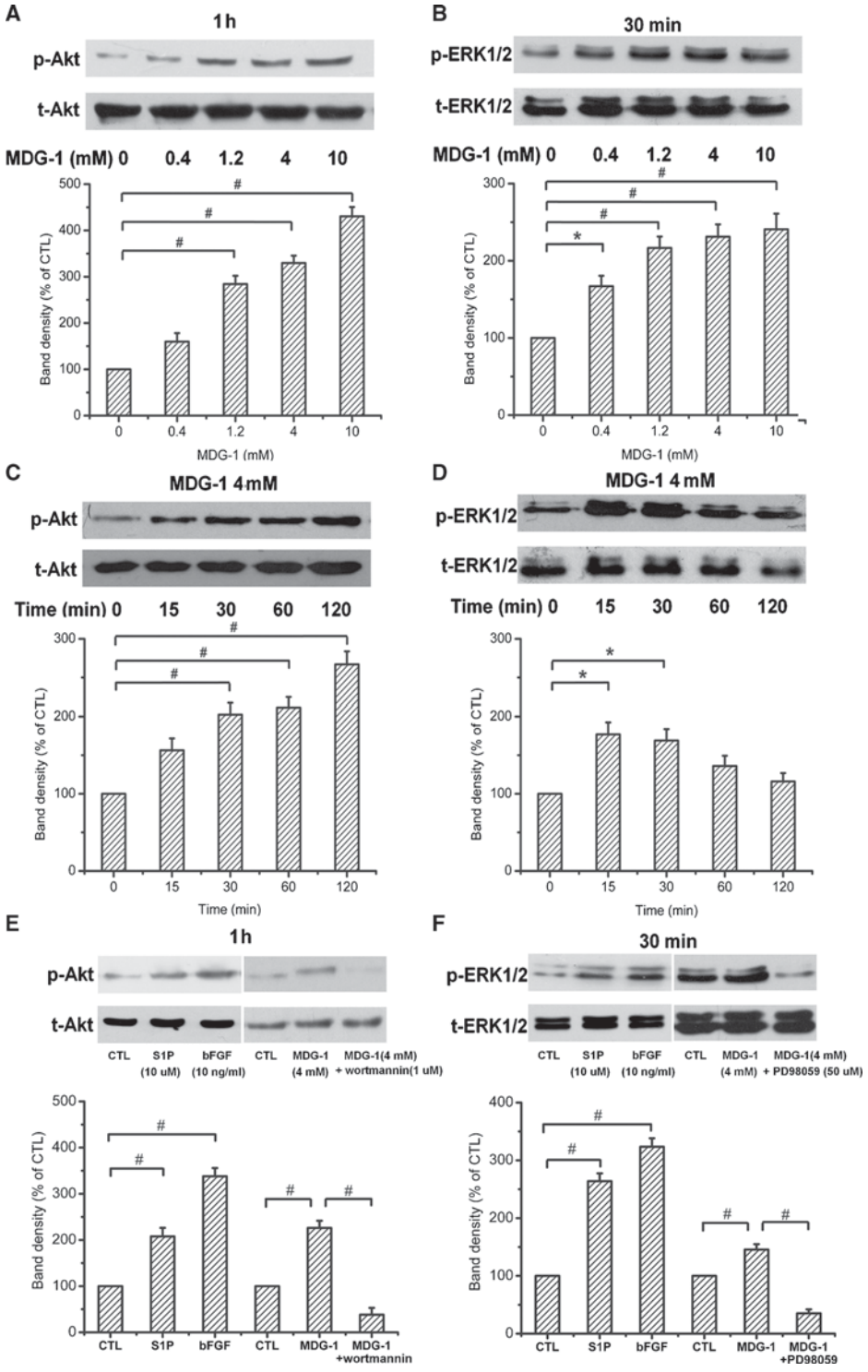

Fig. 5. MDG-1 induces Akt and ERK phosphorylation in HMEC-1 cells. (**A**) HMEC-1 cells incubated with MDG-1 at the indicated concentrations for 1 h were lysed and subjected to Western blotting for phospho-Akt and total Akt. (**B**) HMEC-1 cells incubated with MDG-1 at the indicated concentrations for 30 min were lysed and total ERK and phospho-ERK1/2 was determined. Cells treated with 4 mM MDG-1 for the indicated times were analyzed for the presence of phospho-Akt and total Akt (**C**) or phospho-ERK1/2 and total ERK (**D**). S1P (10 μM) and bFGF (10 ng/mL) treatment has a similar effect on Akt (**E**) and ERK (**F**) phosphorylation. Pretreatment with wortmannin (1 μM) or PD98059 (50 μM) for 1 h abolishes the effects of MDG-1 on Akt and ERk phosphorylation. The band densities for each of the triplicate determinants are shown under the figures. Data are the means ± SD for triplicate experiments ($^{*}P < 0.05$; $^{\#}P < 0.01$).

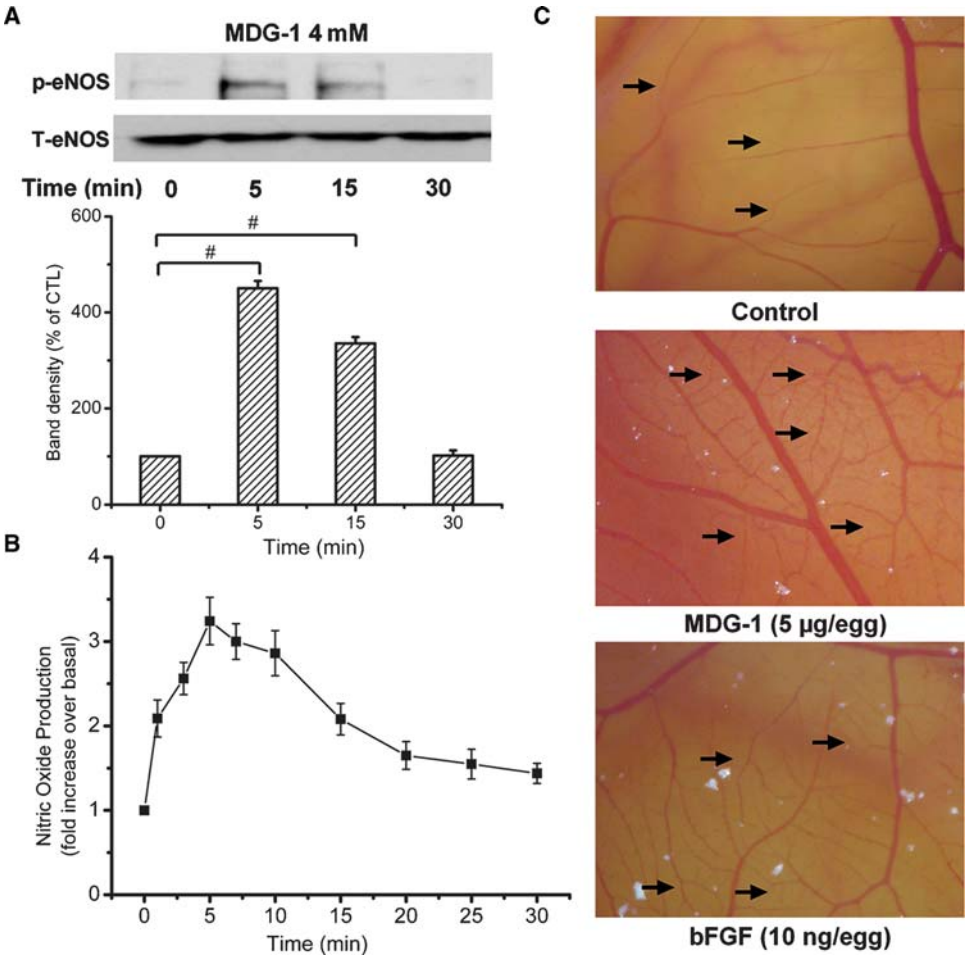

Fig. 6. MDG-1 induces eNOS phosphorylation and stimulates production of NO in HMEC-1 cells, and promotes neovascularization in a CAM assay. (**A**) HMEC-1 cells incubated with 4 mM MDG-1 for 5, 15, or 30 min were lysed and total eNOS and phospho-eNOS was determined. The band densities for each of the triplicate determinants are shown under the figures. (**B**) HMEC-1 cells were incubated with 4 mM MDG-1 for the indicated times, and then the medium was mixed with the Griess reagent. The nitrite concentration was determined at 540 nm by spectrophotometry. Data are the means ± SD for triplicate experiments ($^{*}P < 0.05$; $^{\#}P < 0.01$). (**C**) CAM were treated with saline as control, 5 μg/egg of MDG-1, or 10 ng/egg of bFGF for 48 h; the zones of neovascularization were photographed. Arrows show new vessels forming in CAM. Similar results were obtained from three independent experiments ($n = 10$).

with 10 μM S1P and 10 ng/mL bFGF. Meanwhile, MDG-1-induced Akt and ERK phosphorylation was abolished by 1 μM wortmannin and 50 μM PD98059, respectively (Figure 5E and F).

MDG-1 induces eNOS phosphorylation and stimulates production of NO

Since MDG-1 can stimulate Akt phosphorylation and NO can mediately stimulated angiogenesis, we test whether MDG-1 can increase eNOS phosphorylation and stimulate production of NO in HMEC-1 cells. A single dose of MDG-1 (4 mM) induced a time-dependent increase in eNOS phosphorylation which peaked at 5 min and lasted until 15 min (Figure 6A). When HMEC-1 cells were treated with MDG-1, we observed a significant 3-fold increase in production of NO with a distinct time course (Figure 6B).

MDG-1 promotes neovascularization in a CAM assay

The proangiogenic activity of MDG-1 was investigated in vivo using a CAM assay, which is a convenient and reproducible test system for evaluating proangiogenic compounds. Initially, 15 eggs were tested with saline as control, 5 μg/egg of MDG-1 and 10 ng/egg of bFGF to ensure that at least 10 viable embryos were assessed. There was a significant increase in CAM neovascularization by the addition of MDG-1 (5 μg/egg), suggesting a proangiogenic effect of MDG-1 in vivo. bFGF (10 ng/egg) also observed significant increase in CAM neovascularization (Figure 6C).

MDG-1 protects cells damage from acute myocardial ischemia in rats

The anti-ischemic effect of MDG-1 was assessed using an in vivo model of acute myocardial ischemia in rats. At the end of the treatment period, the final count of rats was: sham group, 8; acute myocardial ischemia group, 9; positive control bFGF group, 7; MDG-1 (3 mg/kg) group, 8; MDG-1 (9 mg/kg) group, 8; and MDG-1 (30 mg/kg) group, 9. The hearts were removed and processed for HE staining (Figure 7A). There was no pathological change in the sham group (Figure 7C). However, in the acute myocardial ischemia group, the average infarct size

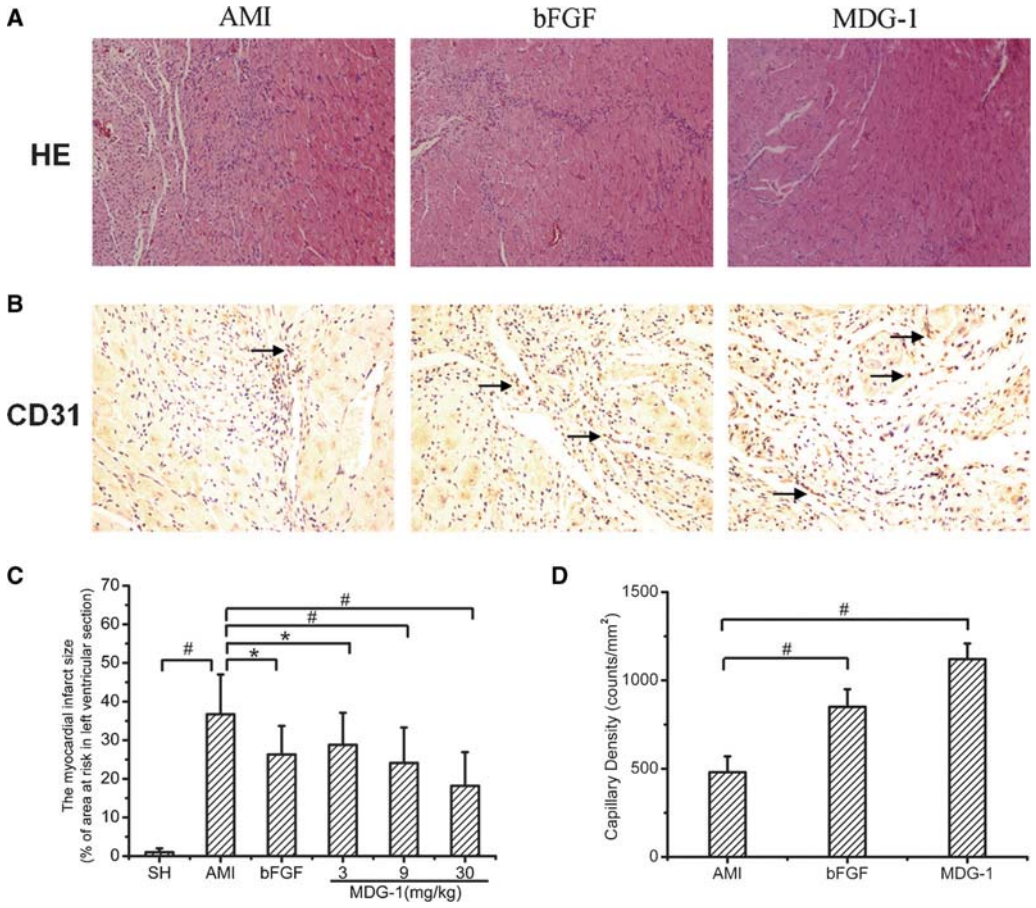

Fig. 7. MDG-1 protects myocardial cells from ischemia-induced damage and promotes angiogenesis in rats in vivo. The anti-myocardial ischemic effects of MDG-1 in vivo were assessed using a model of acute myocardial ischemia in rats as described in *Materials and methods*. (**A**) Representative photomicrographs of HE stained histological slides of the rat hearts are shown from the AMI, bFGF, and MDG-1 groups; the infarct areas are stained with amethyst color by HE. (**C**) Means ± SD of infarct size for five section determinations are shown under the figures ($^{*}P < 0.05$; $^{\#}P < 0.01$). (**B**) Photomicrography shows representative immunohistochemical CD31 staining of ischemic myocardium harvested at day 28. Dots (arrow) indicate capillaries. The images shown are representative of sections obtained from at least five heart samples. (**D**) Effect of MDG-1 on the mean number of capillaries per mm^2 of the infarcted area ($^{\#}P < 0.01$).

was 36.7 ± 10.3% with widespread myocardial cytolysis and coagulative necrosis in the center of the infarct (Figure 7A and C). The bFGF-treated rats had significant myocardial preservation, with an average infarct size of 26.3 ± 7.4% (Figure 7C). In the MDG-1 treated groups, the average infarct size was 28.8 ± 8.3%, 24.1 ± 9.2%, 18.2 ± 8.7% at the concentration of 3, 9, 30 mg/kg, respectively (Figure 7C). The significant decrease in the average infarct size following i.v. administration of MDG-1 suggests a myocardial protective effect in vivo. Meanwhile, the hemodynamics study showed that there were no statistical differences between MDG-1 and AMI group (supplementary Table S1).

Effect of MDG-1 on angiogenesis in ischemic myocardium

To examine the effect of MDG-1 on angiogenesis in ischemic myocardium, immuno-histochemical analysis of CD31-positive cells was performed. As shown in Figure 7B, MDG-1 displayed a significantly higher capillary density in the ischemic border zone at 28 days after ischemic myocardium, similar with the bFGF-treated group. Quantitative analyses of histological sections revealed that MDG-1 significantly increased density of CD31-positive cells compared with controls (Figure 7D). These data showed that MDG-1 promotes neovascularization in ischemic myocardium.

Discussion

It was reported that *Ophiopogon japonicus* polysaccharides might stimulate the proliferation of cultured lymphocytes, exhibited the preventive effect on an autoallergic mouse model for Sjogren's syndrome (Wu et al. 2006; Wang et al. 2007). However, to date, there is little information in the literature concerning the potential anti-ischemic effect and possible mechanism of polysaccharides from *Ophiopogon japonicus.* In the present study, we demonstrate that the polysaccharide MDG-1, extracted from *Ophiopogon japonicus*, protects cardiomyocyte and HMEC-1 cells against OGD-induced cell death, as well as protecting myocardial cells from ischemia-induced death occurring after coronary artery ligation in rats. MDG-1 upregulates SPHK1 and $S1P_1$ expression, induces Akt, ERK, and eNOS phosphorylation and stimulates production of NO, promotes migration and the formation of tube-like structures by HMEC-1 cells, and promotes neovascularization in ischemic

myocardium. Similarly, we found that exogenous S1P enhances HMEC-1 cell tube formation and induces Akt/ERK phosphorylation. Furthermore, both MDG-1 and S1P stimulate bFGF expression in the cells and bFGF can inhibit cell apoptosis and promote proliferation and neovascularization of endothelial cells. These data suggest that MDG-1 presents remarkable anti-ischemic activity and protects cardiomyocyte and HMEC-1 cells from ischemia-induced cell damage by inducing S1P and bFGF cytoprotective and proangiogenic effects via the S1P/bFGF/Akt/ERK/eNOS signaling pathway.

Having established the ability of MDG-1 to prevent ischemia-induced cell death, we investigated the intracellular signaling pathways involved. The involvement of the S1P/bFGF/Akt/ERK/eNOS signaling pathway was confirmed by the effects of Akt and ERK inhibitors, which impaired the MDG-1 cytoprotective effect. Moreover, MDG-1-induced endothelial cell migration and tube formation were also blocked by either wortmannin or PD98059. These data provide evidence that MDG-1 induces its anti-ischemic effect by activating the S1P/bFGF/Akt/ERK/eNOS signaling pathway.

S1P may protect endothelial cells from apoptosis by phosphorylating Akt via the $S1P_1$ receptor (Wang et al. 1999; Limaye et al. 2005). SPHK1 is the anti-apoptotic isoform of sphingosine kinase, which catalyzes S1P production (Waeber et al. 2004). In this study, we found that S1P treatment promotes tube formation and increases Akt and ERK phosphorylation in HMEC-1 cells. Both wortmannin and PD98059 reduced S1P-induced Akt and ERK phosphorylation. These data suggest that MDG-1 activates the S1P signaling pathway by upregulating the expression of SPHK1 and $S1P_1$, which promotes the secretion of S1P. As the downstream signaling effectors of S1P, both Akt and ERK are crucial in endothelial cell angiogenesis. Activation of Akt and ERK by extracellular signals increases endothelial cell survival, proliferation, migration, tube formation, and neovascularization (Secchiero et al. 2003; Kawasaki et al. 2003; Munoz-Chapuli et al. 2004; Calabro et al. 2004). In addition, NO has recently been added to the list of endogenous mediators of angiogenesis, it has been shown that NO mediately stimulated angiogenesis (Gallo et al. 1998). The present study shows that MDG-1 induces phosphorylation of Akt and ERK in a dose- and time-dependent manner, and MDG-1 induces phosphorylation of eNOS and stimulates production of NO. Combined with the data above, it suggests that the S1P/bFGF/Akt/ERK/eNOS signaling pathway indeed has a clear role in MDG-1-induced cytoprotection and angiogenesis. However, the mechanism by which MDG-1 activates the S1P/bFGF/Akt/ERK/eNOS signaling pathway requires further investigation.

bFGF is the main factor which promotes proliferation and neovascularization of endothelial cells by binding with the FGF receptors. Interestingly, activation of bFGF can also inhibit endothelial cell apoptosis (Karsan et al. 1997; Munoz-Chapuli et al. 2004). Indeed, the present data suggest a role for bFGF in mediating the anti-ischemic effect of MDG-1. On the other hand, since MDG-1 upregulates bFGF and activates S1P signaling pathway, and both MDG-1 and S1P can promote tube formation, it is possible that there is crosstalk between the S1P signaling pathway and bFGF in HMEC-1 cells. We found that both S1P and MDG-1 upregulate the expression of bFGF; however, bFGF had no effect on either SPHK1 or $S1P_1$ expression in HMEC-1 cells. These data suggest that MDG-1 increases bFGF expression levels through the S1P signaling pathway in HMEC-1 cells. Since bFGF is an important growth factor involved in the Akt/ERK signaling pathway and may induce Akt/ERK phosphorylation in HMEC-1 cells, the anti-ischemia effect of MDG-1 is probably mediated by initiating a cell signaling cascade through the S1P/bFGF/Akt/ERK/eNOS signaling pathway.

In summary, the present study provides the first evidence of, and a possible explanation for, the cytoprotective and proangiogenic effect of MDG-1 administered exogenously. This effect is mediated by activation of the S1P/bFGF/Akt/ERK/eNOS signaling pathway. Additional work is required to understand comprehensively the anti-ischemia potential and mechanism of action of MDG-1. Considering the activities already identified and the traditional use of this medicinal species, the data presented in this report may be valuable to the development of this carbohydrate-based drug.

Material and methods

MDG-1 was prepared by extraction from the tube root of *Ophiopogon japonicus* (Cixi, Zhejiang province, China) and purification as described previously (Xu et al. 2005). Briefly, tuberous roots of *Ophiopogon japonicus* were extracted with 10 vols. of water at 95∼100°C followed by dialysis. The concentrated dialyzed extract was precipitated by 4 vols. of 95% EtOH. The resulting precipitate was redissolved and centrifuged. The supernatant was lyophilized to obtain crude polysaccharide. The crude product was further purified using the ultrafiltration membrane (*Mw* cut-off was 10,000) under pressure of 0.3 *MPa*. A portion of the products with molecular weight estimated less than 10,000 was fractionated on DEAE Sepharose FF eluted with H_2O. The major fraction was pooled, dialyzed, concentrated, lyophilized, and followed by purification using the Sephadex G-25 column eluted with H_2O to obtain MGD-1. MGD-1 is a water-soluble white powder. The solubility of MDG-1 in H_2O, MeOH, EtOH is 140.2, 2.6 and 0.15 g/L, respectively; The specific rotation ($[\alpha]^{20}_D$) was $-20.66°$ (0.5, H_2O) (unpublished data).

The cell culture medium MCDB131, fetal bovine serum (FBS), and all other cell culture supplements were purchased from GIBCO-BRL (Grand Island, NY). The antibody against SPHK1 was purchased from Abnova (Taiwan), while those against phosphorylated ERK (Thr202/Tyr204), total ERK, phosphorylated Akt, total Akt, phosphorylated eNOS, total eNOS and basic fibroblast growth factor (bFGF) were from Cell Signaling Technology (Beverly, MA), and the antibody against $S1P_1$ was from Affinity BioReagents (Golden, CO). The ERK inhibitor PD98059, Akt inhibitor wortmannin, and fibroblast growth factor receptor (FGFR) inhibitor Su5402 were obtained from Calbiochem (San Diego, CA). Matrigel was purchased from BD Biosciences (Bedford, MA). For secondary antibodies, we used either peroxidase-conjugated goat anti-rabbit IgG or peroxidase-conjugated goat anti-mouse IgG from Jackson Immunoresearch (West Grove, PA).

Cell culture and oxygen glucose deprivation (OGD)

Human microvascular endothelial cells (HMEC-1) were maintained in the MCDB131 medium containing 10% FBS (v/v), 2 mM L-Glutamine, 5 ng/mL epidermal growth factor (EGF), and antibiotics (100 U/mL penicillin, 100 μg/mL streptomycin) at 37°C in a 5% CO_2 incubator. Cardiomyocytes from 1- to

3-day-old neonatal Sprague–Dawley rats were isolated and cultured as described (Nebigil et al. 2003). Cells were maintained in MEM supplemented with 10% FBS and antibiotics (100 U/mL penicillin, 100 μg/mL streptomycin) at 37°C in a 5% CO_2 incubator. For OGD, HMEC-1 and cardiomyocytes cells were cultured in 96-well tissue culture plates (1.5×10^4 cells/well) for 24 h. The cells were transferred into a temperature-controlled ($37° \pm 1°C$) anaerobic chamber (BioSpherix, NY) containing a gas mixture of 5% CO_2 and 95% N_2, and incubated in a glucose-free Hank's balanced salt solution (116 mmol NaCl, 5.4 mmol KCl, 0.8 mmol $MgSO_4$, 1 mmol NaH_2PO_4, 0.9 mmol $CaCl_2$, 10 mg phenol red, pH 7.4). The oxygen levels in the chamber were near complete anoxia (<0.8% oxygen). Cells were maintained in the chamber under OGD conditions with different concentrations of MDG-1 for 8 h to induce injury. The control cell cultures were maintained in the standard culture medium for the same time period in a 5% CO_2 incubator.

Cell death assays

HMEC-1 cells cultured in 96-well tissue culture plates (1×10^4 cells/well) with 10% FBS for 24 h were exposed to different concentrations of MDG-1 for another 24 h. Cell viability was measured by the 3-(4, 5-dimethylthiazol-2-yl)-2, 5-diphenyltetrazolium bromide (MTT) method according to the manufacturer's instructions (Dingguo Company, Beijing, China).

After the HMEC-1 and cardiomyocyte cells were exposed to MDG-1 (0.4, 1.2, 4, and 10 mM) under OGD for 8 h, the medium in individual wells was collected and centrifuged to remove dead cells. Lactate dehydrogenase (LDH) activity in the supernatant was measured using the CytoTox 96 kit (Promega, Madison, WI) according to the manufacturer's instructions. For treatment with the inhibitors, HMEC-1 cells were pretreated with PD98059 (50 μM) or wortmannin (1 μM) for 1 h prior to MDG-1 and OGD exposure. The percentage of cell death was determined by comparing LDH release to values obtained from fully lysed cells.

Scratch wound migration assay

HMEC-1 cells were cultured in 6-well tissue culture plates (5×10^5 cells/well) for 24 h. Then, the confluent monolayer was scraped with a yellow pipette tip to generate a wound and rinsed twice with the growth medium. The cells were photographed immediately after the scratch and 24 h later with an Olympus IX51 digital camera (Tokyo, Japan). The wound area was measured to determine cell migration. The wound size was determined by measuring the distance from one wound edge to the opposing edge, while the edge was identified by focusing on cells which had migrated farthest while still in contact with other endothelial cells.

Tube formation on Matrigel

Culture plates (96 well) were coated with 50 μL Matrigel and incubated at 37°C for 45 min to allow the Matrigel to solidify. HMEC-1 cells pretreated for 1 h with either vehicle or inhibitors (PD98095, wortmannin or Su5402), were plated at a density of 3×10^4 cells/well with test substances or vehicle, and incubated at 37°C for 16 h. The cells were photographed using the Olympus digital camera. Tube formation was quantified by measuring the length of capillary structures in pixels using NIH ImageJ software. Branching points were counted manually. Five randomly selected fields of view were photographed in each well, and averaged to determine the value for each sample.

Angiogenesis antibody array analysis

The expression of 19 cytokines was evaluated using TranSignal Angiogenesis Antibody Arrays (Panomics, Redwood City, CA). HMEC-1 cells were seeded (5×10^5 cells/well) in 6-well plates. After MDG-1 stimulation, cells were lysed with an equal volume of the RIPA buffer [0.5% Triton-X 100, 0.5% deoxycholic acid sodium salt, 0.1% sodium dodecyl sulfate (SDS) and 1% phenylmethylsulfonylfluoride (PMSF), and 1% proteinase inhibitor cocktail (Sigma, St. Louis, MO)] to obtain the protein sample. The membranes were exposed to the blocking buffer for 1 h at 25°C, and incubated the protein sample for up to 2 h at 25°C. After washing three times, the arrays were processed with a biotin-conjugated angiogenesis antibody mix and streptavidin–horseradish peroxidase conjugate according to the manufacturer's protocol.

Western blotting assay

Cells were uniformly seeded (5×10^5 cells/well) in 6-well plates. After MDG-1 stimulation for different periods of time, cells were lysed with an equal volume of the RIPA buffer. Protein concentration was determined by the protein assay (BioRad, Hercules, CA). Total cellular protein (30 μG) was subjected to 10% SDS–polyacrylamide gel electrophoresis and transferred to polyvinyl difluoride (PVDF) membranes. After blocking with Tris-buffered saline with Tween-20 (TBST) containing 5% nonfat milk for 1 h, the membrane was probed for SPHK1, $S1P_1$, phospho-ERK1/2, total ERK1/2, phospho-Akt, total Akt, phosphorylated eNOS, total eNOS or bFGF overnight at 4°C. After incubation with the appropriate secondary antibody for 1 h, the Pierce ECL Western Blot Substrate (Rockford, IL) was used for detection.

Measurement of NO Synthesis

HMEC-1 cells were stimulated with MDG-1 for 1, 3, 5, 7, 10, 15, 20, 25, or 30 min and then the supernatant was collected. The generation of NO was determined by measuring the stable NO metabolites, i.e., total nitrites, in the culture medium with a nitrite detection kit (Beyotime Biotech Inc, Jiangsu, China). Briefly, 30 μL of medium was mixed with 30 μL of Griess reagent in a 96-well plate. Nitrite concentration was determined by spectrophotometry (540 nM) from a standard curve (0–100 μmol/L) derived from $NaNO_2$.

Chick allantoic membrane assay

The chick allantoic membrane (CAM) assay was carried out essentially as described (Tanaka et al. 1986). Fertilized eggs were incubated in a humidified egg incubator for 7 days. On the seventh day, a small orifice was made on the broad side of the egg and a window was carefully created through the eggshell. Squares of Whatman filter paper (5×5 mm) were soaked with 5 μL of normal saline containing 5 μG MDG-1 and then implanted on the CAM. bFGF (10 ng/egg) similarly applied served as a positive control. The windows were sealed with an adhesive tape and the eggs were incubated for another 48 h, during which time nonviable eggs were discarded. The zones of neovascularization under and around the filter paper were photographed using an anatomic microscope (Shanghai, China).

Five randomly selected fields of view were photographed in each egg, and averaged to determine the value for each sample.

Coronary artery ligation and immunohistochemistry

Male Sprague–Dawley rats (100 total; 6–8 weeks old, body weight 270 ± 30 *g*) were housed and used in accordance with the U.S. National Institutes of Health *Guide for the Care and Use of Laboratory Animals* (NIH Manual 3040–2 (1999)), and all procedures were approved by Shanghai University of Traditional Chinese Medicine ethics board. Rats were randomly divided into groups: a negative control (sham operation; normal saline) and four different treatment groups, all of which were subjected to acute myocardial ischemia but treated differently: normal saline, MDG-1 (3 mg/kg i.v.), MDG-1 (9 mg/kg i.v.) or MDG-1 (30 mg/kg i.v.) and a positive control (immediately after ligation, 10 μg of bFGF was injected directly into the ligation zone and myocardium around the ischemic border zone, respectively). Rats were anesthetized by intraperitoneal injection of sodium pentobarbital (30 mg/kg), after which the paraconal interventricular branch of the left coronary artery (corresponding to the left anterior descending coronary artery in humans) was ligated. Control animals underwent a sham operation, in which the incision was made but no ligation was performed. After surgery, the rats were kept on their treatment protocols for 4 weeks. The animals were sacrificed after drug treatment for 1 h, and their hearts were harvested. Hearts were excised and placed in 10% phosphate-buffered formalin. The gross infarct size was estimated in the intact heart by comparison of the length and width of the myocardial infarction and left ventricular areas. Then, the fixed tissue was embedded in paraffin and serially cut from the apex to the level just below the coronary artery ligation site. These sections were stained with hematoxylin (HE). The average infarct size, expressed as a percentage of the area at risk in the left ventricular tissue, was calculated on histological slides by measuring both the perimeter and the area using LEICA workstation software (Leica, Solms, Germany). The infarct size of all sections was averaged and expressed as the percentage myocardial infarction size for each heart. Capillary density was assessed by counting cells staining for the endothelial antigen CD31 in high-power fields and deriving an average value. Briefly, all paraffin sections were incubated overnight at 4°C with rabbit anti-mouse CD31 (1:100, Boster, Wuhan, Hubei province, China). The sections were then washed and incubated with secondary antibodies for 30 min. Diaminobenzidine (DAB) was used to reveal the immunostaining. CD31-positive capillaries were counted in four randomly chosen low power (×100) microscopic fields.

Funding

National Natural Science Foundation of China (grant number 30371685, 30670470, 30770484); the National High Technology Research and Development Program (863) of china (grant number 2006AA022102); and Shanghai Rising-Star Program (grant number 07QA14050).

Acknowledgements

The authors thank Zhongqi Pharmaceutical Technology (SJZ) Co. Ltd of CSPC and Dr Qing-Zhong Jia for the assistance of rat experiments.

Supplementary Data

Supplementary data for this article is available online at http://glycob.oxfordjournals.org/.

Conflict of interest statement

None declared.

Abbreviations

HMEC-1, Human microvascular endothelial cells-1; OGD, oxygen glucose deprivation; S1P, sphingosine 1-phosphate; SPHK1, sphingosine kinase-1; S1P1, sphingosine 1-phosphate receptor 1; ERK, extracellular signalregulated kinase; eNOS, endothelial nitric-oxide synthase; FGF, fibroblast growth factor; CAM, chorioallantoic membrane; SH, sham operation; AMI, acute myocardial ischemia.

References

Bullard LE, Qi X, Penn JS. 2003. Role for extracellular signal responsive kinase-1 and -2 in retinal angiogenesis. *Invest Ophthalmol Vis Sci*. 44:1722–1731.

Calabro P, Samudio I, Willerson JT, Yeh ET. 2004. Resistin promotes smooth muscle cell proliferation through activation of extracellular signal-regulated kinase 1/2 and phosphatidylinositol 3-kinase pathways. *Circulation*. 110:3335–3340.

Carmeliet P. 2003. Angiogenesis in health and disease. *Nat Med*. 9:653–660.

Gallo O, Masini E, Morbidelli L, Franchi A, Fini-Storchi I, Vergari WA, Ziche M. 1998. Role of nitric oxide in angiogenesis and tumor progression in head and neck cancer. *J Natl Cancer Inst*. 90:587–596.

Huang HC, Ni Z. 2003. Effect of *Ophiopogonis* on the auricular microcirculation in mice. *J Shanghai Lab Animal Sci*. 23:57–58.

Jin ZQ, Goetzl EJ, Karliner J. 2004. Sphingosine kinase activation mediates ischemic preconditioning in murine heart. *Circulation*. 110:1980–1989.

Jin ZQ, Karliner JS, Vessey DA. 2008. Ischemic postconditioning protects isolated mouse hearts against ischemia/reperfusion injury via sphingosine kinase isoform-1 activation. *Cardiovas Res*. 79:134–140.

Jin ZQ, Zhou HZ, Zhu P, Honbo N, Mochly-Rosen D, Messing RO, Goetzl EJ, Karliner JS, Gray MO. 2002. Cardioprotection mediated by sphingosine-1-phosphate and ganglioside GM-1 in wild-type and PKC epsilon knockout mouse hearts. *Am J Physiol Heart Circ Physiol*. 282:1970–1977.

Karsan A, Yee E, Poirier GG, Zhou P, Craig R, Harlan JM. 1997. Fibroblast growth factor-2 inhibits endothelial cell apoptosis by Bcl-2-dependent and independent mechanisms. *Am J Pathol*. 151:1775–1784.

Kawasaki K, Smith RS, Hsieh CM, Sun J, Chao J, Liao JK. 2003. Activation of the phosphatidylinositol 3-kinase/protein kinase Akt pathway mediates nitric oxide-induced endothelial cell migration and angiogenesis. *Mol Cell Biol*. 23:5726–5737.

Kennedy SG, Wagner AJ, Conzen SD, Jordan J, Bellacosa A, Tsichlis PN, Hay N. 1997. The PI 3-kinase/Akt signaling pathway delivers an anti-apoptotic signal. *Genes Dev*. 11:701–713.

Lee OH, Kim YM, Lee YM, Moon EJ, Lee DJ, Kim JH, Kim KW, Kwon YG. 1999. Sphingosine 1-phosphate induces angiogenesis: Its angiogenic action and signaling mechanism in human umbilical vein endothelial cells. *Biochem Biophys Res Commun*. 264:743–750.

Limaye V, Li X, Hahn C, Xia P, Berndt MC, Vadas MA, Gamble JR. 2005. Sphingosine kinase-1 enhances endothelial cell survival through a PECAM-1-dependent activation of PI-3K/Akt and regulation of Bcl-2 family members. *Blood*. 105:3169–3177.

Luttun A, Carmeliet G, Carmeliet P. 2002. Vascular progenitors: From biology to treatment. *Trends Cardiovasc Med*. 12:88–96.

Maceyka M, Payne SG, Milstien S, Spiegel S. 2002. Sphingosine kinase, sphingosine-1-phosphate, and apoptosis. *Biochim Biophys Acta*. 1585:193–201.

Miura S, Tanigawa H, Matsuo Y, Fujino M, Kawamura A, Saku K. 2003. Ras/Raf1-dependent signal in sphingosine-1-phosphate-induced tube

formation in human coronary artery endothelial cells. *Biochem Biophys Res Commun*. 306:924–929.

Munoz-Chapuli R, Quesada AR, Angel Medina M. 2004. Angiogenesis and signal transduction in endothelial cells. *Cell Mol Life Sci*. 61:2224–2243.

Nebigil CG, Etienne N, Messaddeq N, Maroteaux L. 2003. Serotonin is a novel survival factor of cardiomyocytes: Mitochondria as a target of 5-HT_{2B} receptor signaling. *FASEB J*. 17:1373–1375.

Secchiero P, Gonelli A, Carnevale E, Milani D, Pandolfi A, Zella D, Zauli G. 2003. TRAIL promotes the survival and proliferation of primary human vascular endothelial cells by activating the Akt and ERK pathways. *Circulation*. 107:2250–2256.

Spiegel S, Milstien S. 2003. Sphingosine-1-phosphate: An enigmatic signaling lipid. *Nat Rev Mol Cell Biol*. 4:397–407.

Tanaka NG, Sakamoto N, Tohgo A, Nishiyama Y, Ogawa H. 1986. Inhibitory effects of anti-angiogenic agents on neovascularization and growth of the chorioallantoic membrane (CAM). The possibility of a new CAM assay for angiogenesis inhibition. *Exp Pathol*. 30:143–150.

Vessey DA, Kelley M, Li L, Huang Y, Zhou H, Zhu BQ, Karliner JS. 2006. Role of sphingosine kinase activity in protection of heart against ischaemia reperfusion injury. *Med Sci Monit*. 12:318–324.

Waeber C, Blondeau N, Salomone S. 2004. Vascular sphingosine-1-phosphate $S1P_1$ and $S1P_3$ receptors. *Drug News Perspect*. 17:365–382.

Wang F, Van Brocklyn JR, Hobson JP, Movafagh S, Zukowska-Grojec Z, Milstien S, Spiegel S. 1999. Sphingosine 1-phosphate stimulates cell migration through a G(i)-coupled cell surface receptor. Potential involvement in angiogenesis. *J Biol Chem*. 274:35343–35350.

Wang Y, Yan TT, Shen J, Guo HY, Xiang XR. 2007. Preventive effect of *Ophiopogon japonicus* polysaccharides on an autoallergic mouse model for Sjogren's syndrome by regulating the Th1/Th2 cytokine imbalance. *J Ethnopharmacol*. 114:246–253.

Ware A, Simons M. 1997. Angiogenesis in ischemic heart disease. *Nat Med*. 3:158–164.

Wu XM, Dai H, Huang LX, Gao XM, Tsim KW, Tu PF. 2006. A fructan, from *Radix Ophiopogonis*, stimulates the proliferation of cultured lymphocytes: Structural and functional analyses. *J Nat Prod*. 69:1257–1260.

Xu DS, Feng Y, Lin X, Deng HL, Fang JN, Dong Q. 2005. Isolation, purification and structural analysis of a polysaccharide MDG-1 from *Ophiopogon Japonicus*. *Acta Pharm Sin*. 40:636–639.

Zheng Q, Feng Y, Xu DS, Lin X, Chen YZ. 2009. Influence of sulfation on anti-myocardial ischemic activity of *Ophiopogon japonicus* polysaccharide. *J Asian Nat Prod Res*. 11:306–321.

Zhou YH, Xu DS, Feng Y, Fang JN, Xia HL, Liu J. 2003. Effects on nutrition blood flow of cardiac muscle in mice by different extracts in radix *Ophiopogonis*. *Chin J Exp Tradit Med Form*. 9:22–23.